energies

MDPI

*Article*

# Effects of the Heat Transfer Fluid Selection on the Efficiency of a Hybrid Concentrated Photovoltaic and Thermal Collector

**Catarina Sofia Campos [1], João Paulo N. Torres [2,*] and João F. P. Fernandes [3]**

[1] Instituto Superior Técnico, Universidade de Lisboa, 1649-004 Lisboa, Portugal; catarina.s.campos@ist.utl.pt
[2] Instituto de Telecomunicações, Instituto Superior Técnico, Universidade de Lisboa, 1649-004 Lisboa, Portugal
[3] Institute of Mechanical Engineering (IDMEC), Instituto Superior Técnico, Universidade de Lisboa, 1649-004 Lisboa, Portugal; joao.f.p.fernandes@tecnico.ulisboa.pt
* Correspondence: joaotorres@tecnico.ulisboa.pt

Received: 1 March 2019; Accepted: 21 April 2019; Published: 13 May 2019


**Abstract:** This work focuses on the performance study of the PowerCollector™, a concentrated photovoltaic thermal system with a custom-made geometry and a photovoltaic cell cooling technology. To do so, a model that portrays the behavior of this concentrating solar system was developed. In order to validate all the information obtained with its simulation, measurements were taken from an experimental setup and were compared to the respective results predicted by this exact same model. It should be noted that all these procedures were based on the fluid for which the PowerCollector™ has been designed (water). Hence, the efficiency enhancement using nanofluids was also considered, as data from some studies addressing this issue were analyzed. Alongside all of this, the corrosion and erosion effects on the pipes incorporated in this system and originated by all the fluids mentioned throughout this investigation were also evaluated. In summary, with this entire study, it could be concluded that nanofluids may represent an appropriate alternative to water, as long as they are chosen according to all particularities of each case.

**Keywords:** corrosion; electrical and thermal efficiency; nanofluid; PowerCollector™

## 1. Introduction

The production of electricity through solar energy is a well-known process. The first product capable of transforming solar radiation into electricity, using the photoelectric effect, was discovered by Edmond Becquerel in 1877 with a conversion efficiency of 0.5%. Since then, solar cell technology had changed and nowadays the available solar panels in the market have an efficiency of around 22.5%, with some companies, such as Panasonic, proclaiming to have reached such levels [1].

Research dates further back when regarding the use of the energy that arrives from the Sun as a source to produce heat. This began with the Swiss scientist Horace Saussure in 1767 [2]. He performed an experiment in which to heat water he put the liquid inside a black painted box and then the box in another case made of glass and thermally shielded it. With this method, the water reached a temperature of 109 °C. In 1908, William Bailey [3] presented a patent for a water heater that is quite similar to the solar collectors produced nowadays. For the first time, with this discovery, it was possible to separate the energy storage from the heating part of the system. The separation of the system in two parts reduced heat loss during the night [4]. Modern solar collectors can reach levels of efficiency between 70 and 90%.

Due to the continuous development of solar technology, the use of the solar panel to produce only electricity was beaten. It was announced that a new form of generation in which the heat generation

was added to the electricity production, thus creating hybrid panels, which are both photovoltaic and thermal (PVT).

Unifying the thermal and the electric sides, the hybrid panels have to reach a compromise between the two technologies. It is quite impossible to maximize these two aspects at the same time and a different way to use energy from the Sun had to be found. With the adoption of this technology, it is possible to obtain an improvement of the photovoltaic cell's efficiency of about 50%. The possibilities unlocked by PVT technology are underlined from achievements such as reaching 44.5% efficiency, using the new PV panels containing gallium antimonide (GaSb) [5].

The concentrated photovoltaic-thermal (C-PVT) panel has three different possible configurations: the first one, a low concentration PVT (LCPVT), which has a concentration factor between 2 and 100 suns. The second configuration, a medium concentration PV, with a configuration that supports between 100 and 300 suns. The last configuration is a high solar concentration system with a concentration factor higher than 1000 suns (HCPVT) [6]. A Swedish renewable-energy company, SOLARUS, developed the PowerCollector™, a concentrated photovoltaic and thermal (CPVT) system [7].

This CPVT system offers two main technologies that impact its design: An Active Cell Cooling™ (ACC™) technology and a custom-made geometry called MaReCo™, which stands for a Maximum Reflector Collector™. The unique and patented Solarus PowerCollector™ has the highest yield ever measured. Slowly but certainly the market is discovering that this third generation solar is indeed the most efficient way to get energy from the sun, as was already stated by the International Energy Agency years ago. SOLARUS is at the moment the only company in the world, able to produce this technology on a mass scale. The potential for this innovative technology is beginning to show and grow, and since it perfectly meets the needs of hotels, one can benefit from it in other sectors. This makes the Solarus Power Collector the absolute highest performing solar collector on the planet generating three times more energy from a surface than conventional PV-panels. The peak performance of one Power Collector is 1.350 WpThermal and 275 Wp-Electrical.

The latter, whose accurate classification for its shape is asymmetrical parabolic, is responsible for sunlight concentration on the two-lower photovoltaic modules, whereas the former focuses on the heat extraction from the solar cells [8].

This cooling feature involves the use of a heat-transfer fluid (HTF), which in turn plays a significant role in the thermal energy generation as well as in the electrical efficiency of the PowerCollector™ [9–11]. The selection of different fluids as a cooling material is, therefore, expected to impose a relevant impact on the CPVT system efficiency, a subject matter worthy of a detailed analysis throughout this paper.

The main focuses of this research are to reduce the adverse effects in the collector, optimizing the temperature distribution, and trying to develop a study method that could be used to investigate the different problems; such as those caused by the shadings and uneven distribution of the temperature. The electric circuit configuration analysis will surely contribute to more convenient distributions of the electric and thermal energies in the collector. These two aspects, electric and thermal, are undoubtedly interrelated. The bi-directional electric-thermal interactions will be important and will certainly lead to complex questions and problems due to the non-linearity involved.

The paper is organized as follows: Section 1 presented in a brief way the CPVT system configuration developed by SOLARUS and the problem under study. Section 2 addresses the methods and models used. Section 3 evaluates the experimental results obtained using all the concepts mentioned in the previous section and it also validates the developed model. Section 4, on the other hand, introduces and explains some novelties that might be beneficial to the CPVT system efficiency, namely what concerns heat-transfer fluid. In Section 5, conclusions are made.

## 2. The PowerCollector™ Model

As stated in the previous section of this paper, the SOLARUS PowerCollector™ is composed of several elements with a well-defined purpose and a clear effect on its final yield. This means that if one wants to develop an illustrating model of the different heat transfer fluid consequences on this system's

efficiency, it is recommended to divide it by its main features. Therefore, the carried out design of the PowerCollector™ model for this particular study consists of a three-model implementation dependent on the results of each other, as described in the subsequent topics and also in the paper [12].

### *2.1. Optical Collector Model*

One of the main CPVT features is the MaReCo™ technology, responsible for concentrating the sunlight reflected in the concentrator in a limited area at the bottom of the solar panel. This area has a huge influence on the amount of energy generated, so an important step to be taken is to develop an optical collector model that determine the solar irradiance distribution throughout the day. In this model, every technical specification of the system was taken into account and used in the program SolTrace. The SolTrace is a ray tracing software tool where the panel's tilt and exact location are two parameters that need to be defined. Finally, the local day solar hour is also an important factor with a great impact on the concentrated sunlight distribution. In addition to all of this, with the resulting model, it is possible to observe a three-dimensional (3-D) representation of the modeled system with the solar rays' path for the imposed conditions (Figure 1).

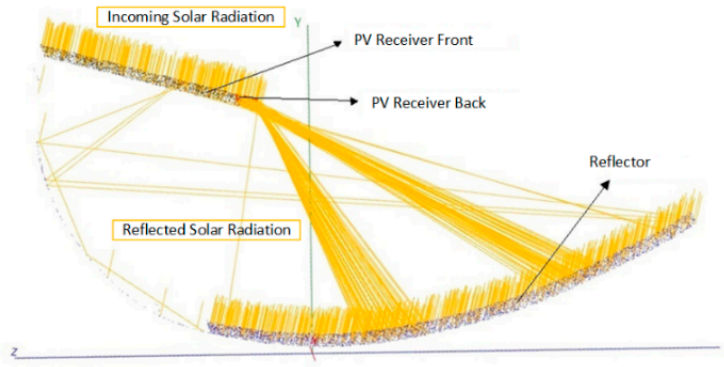


**Figure 1.** 3-D representation of the optical collector model in SolTrace.

### *2.2. Thermal Model*

To acquire the hybrid system thermal component behavior, it is necessary to model the total irradiance that reaches the PV modules, a procedure executed with COMSOL Multiphysics® [13]. Furthermore, regarding the highly non-uniform performance of the received concentrated sunlight and according to all data acquired from the previously described model, the lower PV modules of the simulated CPVT were divided into three sections of uniform irradiance and adjustable width (Figure 2).

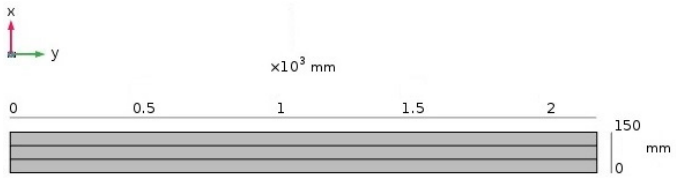


**Figure 2.** Bottom view of a photovoltaic panel.

This model needs to address the entire thermal phenomena related to the heat transferred to the fluid. Thus, it should be known that the thermal energy transmission between the receiving surfaces of solar radiation, and the CPVT can be computed by the following equation [14],

$$\rho C_p u \cdot \nabla T = \nabla \cdot (\kappa \nabla T) + Q \quad (1)$$

where $\rho$ is the solid density in kg/m$^3$, $C_p$ is the solid heat capacity at constant pressure in J/(kg·K), $\kappa$ is the solid thermal conductivity in W/(m·K), $u$ is the fluid velocity field in m/s, $Q$ is the heat source in

W/m$^3$, $T$ is the collector's temperature in K and $q$ is the heat flux in W/m$^2$. It is important to note that Equation (1) describes the thermal conduction phenomena in a steady-state regime, which explains how the HTF extracts all the accumulated heat in the PV panels. The fluid motion, on the other hand, is mathematically depicted by both continuity and Navier–Stokes equations, which can be merged into a single expression for the steady-state regime [15],

$$0 = \nabla \cdot \left[ -pI + \mu\left(\nabla u + (\nabla u)^T\right) - \frac{2}{3}\mu(\nabla u)I \right] + F \tag{2}$$

In the previous equation, $\mu$ is the fluid dynamic viscosity in Pa and $p$, the fluid pressure in Pa. Additionally, for simplification purposes and considering low fluid velocity, it was defined as the fluid flow as being laminar.

It is also important to include the collector's heat transfer with the surrounding environment through natural convection, a mechanism mathematically described as follows [13]:

$$-n \cdot (-\kappa \nabla T) = h(T_{amb} - T) \tag{3}$$

As it can be seen from Equation (3), the heat transfer coefficient, $h$, is a parameter that could be estimated, with equation [14,15],

$$\begin{cases} h = 4V_\infty + 5.6, & V_\infty < 5 \text{ m/s} \\ h = 7.1{V_\infty}^{0.78}, & V_\infty > 5 \text{ m/s} \end{cases} \tag{4}$$

where $V_\infty$ is the wind speed in m/s.

### 2.3. Electric Model

The calculation of the collector's electrical performance is purely based on mathematical equations derived from the 3 parameters and 1 diode model (1M3P), a simplified model in which the non-linear solar cell's, *I–V* (current–voltage) characteristic can be both obtained and explained with an equivalent electric circuit. Regarding this curve, it is possible to underscore the current and voltage values for which the peak power ($I_{MP}$ and $U_{MP}$, respectively) is obtained; this basically consists of ascertaining the point where the power produced by the cell is maximum (MPP). This point changes value with atmospheric conditions, such as irradiance and temperature. The method used by the 1M3P model to acknowledge this issue is based on the definition of several parameters, whose value depends on these two meteorological characteristics. Both $I_{MP}$ and $U_{MP}$ are then computed using these same quantities, resulting in peak power values also variable with irradiance and ambient temperature [16],

$$P = U_{MP} \cdot I_{MP} \tag{5}$$

Given that MPP represents the operating point where the PowerCollector™ should always be working on, the previous equation represents the desired value for the electric power generated. The required irradiance and temperature values to compute it were obtained from the previously mentioned thermal and optical collector models.

#### 2.3.1. Influence of the Temperature

Solar cells become less efficient with the temperature increases, an effect that has repercussions on the electricity generation of the system. In the 1M3P model, one of the main parameters that is affected by the temperature is the thermal voltage ($V_T$), a value used for most of the remaining quantities' computation [16],

$$V_T = \frac{KT}{q} \tag{6}$$

and whose equation shows a variation with the Boltzmann constant, $K$, which is $1.38 \times 10^{-23}$ J/K, the cell's temperature, $T$ in $K$, and the electron charge, $q$, of $1.6 \times 10^{-19}$ C. Nevertheless, when it comes to the electrical influence of the photovoltaic cell's temperature, the diode's reverse saturation current ($I_0$) also plays an important role [16],

$$I_0 = I_0^r \left(\frac{T}{T^r}\right)^3 \exp\left[\frac{\varepsilon \cdot N_S}{m}\left(\frac{1}{V_T^r} - \frac{1}{V_T}\right)\right] \tag{7}$$

In the previous equation, the upper index $r$ represents a standard test condition (STC) parameter, $\varepsilon$ is the band gap (1.12 eV for silicon), $m$ is the diode's ideality factor and $N_S$ is the number of cells in series.

#### 2.3.2. The Influence of the Irradiance

In a solar cell, it is possible to observe an increase in the generated electrical power with increases of solar radiation. The short-circuit current ($I_{SC}$) is the parameter that describes this effect on the cell's performance with the following equation [16],

$$I_{sc} = \frac{G}{G^r} I_{sc}^r \tag{8}$$

where $G$ is the irradiance reaching the solar cells in W/m$^2$.

#### 2.3.3. Constant Parameter and Final Computations

There is also another important parameter that does not depend on any atmospheric condition, the diode's ideality factor ($m$). Its calculation requires the use of only the values given in the manufacturer datasheet, as it can be seen from Equation [16].

$$m = \frac{U_{MP}^r - U_{oc}^r}{V_T^r \ln\left(1 - \frac{I_{MP}^r}{I_{sc}^r}\right)} \tag{9}$$

Once all these calculations are concluded, it is possible to achieve the $I_{MP}$ and $U_{MP}$ with the use of the following pair of equations, which are solved iteratively [16]:

$$\begin{cases} U_{MP}^{(k+1)} = m V_T \ln\left(\frac{\frac{I_{sc}}{I_0} + 1}{\frac{U_{MP}^k}{m V_T} + 1}\right) \\ I_{MP} = I_{sc} - I_0\left(e^{\frac{U_{MP}}{m V_T}} - 1\right) \end{cases} \tag{10}$$

As the $U_{MP}$ equation is non-linear, its resolution should be done with an iterative method where $U_{MP}^r$ is the reference value.

## 3. Simulation Model Validation

To validate the developed model, a set of experiments were performed on a PowerCollector™ installed on the Taguspark terrace. The main goal of the experimental tests was to measure the CPVT's electrical performance throughout a summer day in which the PV modules were either cooled or non-cooled. The comparison between all the obtained data and the respective results predicted by the model will determine how well this same model can depict an actual PowerCollector ™ setup.

In this case, besides the CPVT location, there are also some other parameters that must be carefully chosen to get the best performance of the photovoltaic system. The collector's orientation and the solar panel's tilt, for instance, are two parameters with a huge importance that affect the system efficiency crucially. In Portugal, considering the results of some studies carried out over the years, solar

panels facing south is the most common alternative used and, based on this, the chosen orientation for the future setup was also south. Furthermore, to choose the best tilt for the desired configuration, an in-depth study of the absorbed solar power variation with this parameter was estimated for every month of the year. With all the obtained data, an attempt was made to choose a value at which the concentration effect is boosted throughout the year and, after some analysis, that value was found to be 15.6°.

For the thermal installation, a pipe with a water flow of 0.5 $m^3$/h was connected to one of the system sides, whereas the other half received the cooling fluid through a connecting thermal fitting. In relation to the electrical installation [7] the two sides were connected in series and the output current and voltage were measured using an ammeter and multimeter, respectively. The connection between the collector and the grid was done with a maximum power point tracker (MPPT), a device responsible for the desired MPP operation. Moreover, a pyranometer and a temperature sensor were also used on the experiments to measure the actual irradiance reaching the upper PV modules and the ambient temperature, respectively.

With this setup (Figure 3), two experimental tests were done in an alternating manner. On the first one, voltage and current measurements were carried out on specific hours of the day without any PV cell cooling. On the second one, however, an extra temperature sensor was used to measure the output and input fluid's temperature, meaning that in this case the same procedure was executed but with the ACC™ technology also included.

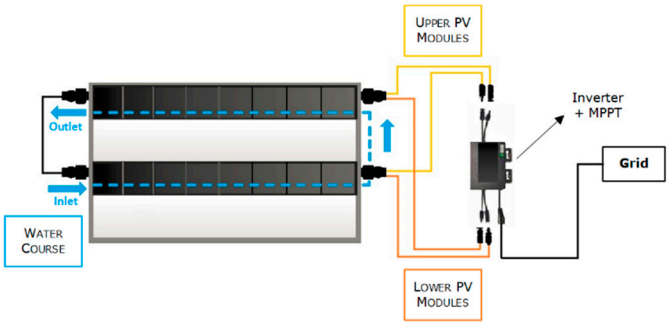


**Figure 3.** Schematics of the PowerCollector™ electrical installation.

*Experimental Results*

From the acquired voltage and current values for each hour, the electrical power produced by the panels were determined. A wattmeter included in the setup also registered the evolution of these parameters throughout the entire experiment (Figure 4).

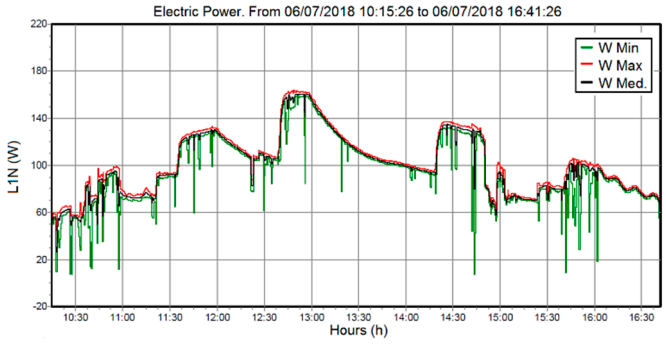


**Figure 4.** Electric power evolution obtained throughout the entire experiment.

As can be seen from Figure 4, at specific moments of the day, there are some abrupt changes in the power generated. The reason for this is related to the HTF flow, which has a positive impact every time it is incorporated in the system and a negative one when the fluid stops flowing through the cooling tubes

Even though the concentration factor is less than 1, the results for both experimental tests, with and without the cooling technology, are shown in Figure 5a,b. This figure shows the concentration effect on the lower PV modules and also an improvement of the performance of the cell when they are cooled down.

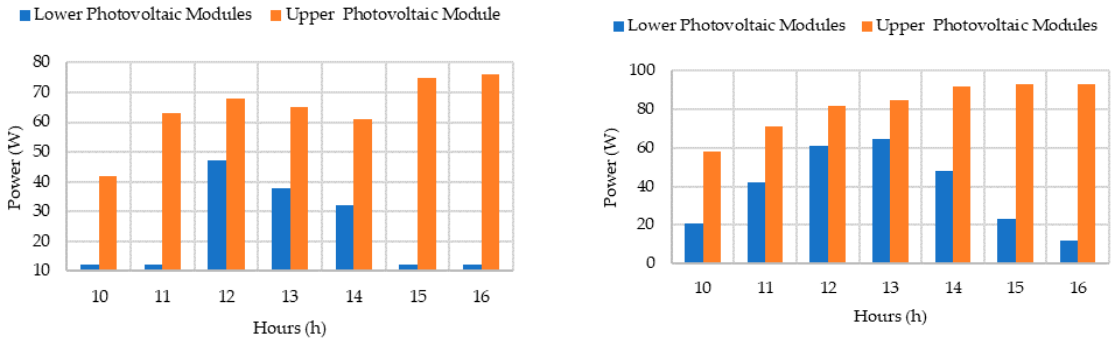


(**a**) (**b**)

**Figure 5.** Electric power produced by each PowerCollector™ panel in the: (**a**) non-cooling system and (**b**) in the cooling system.

The small difference between the fluid's initial and final temperature should also be mentioned, Figure 6, because that is only possible on a steady-state regime, simulated during the experiment to obtain experimental results as close as possible to the predicted ones.

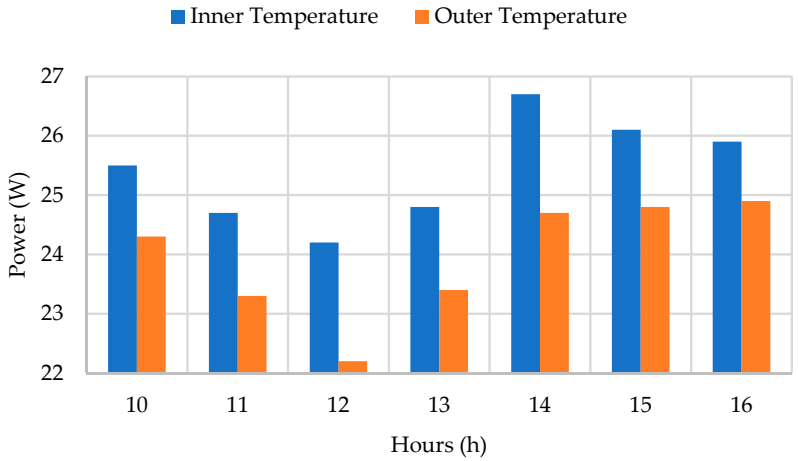


**Figure 6.** The inner and outer temperature of the water.

As stated before, after the experimental tests, the same conditions were simulated using the PowerCollector™ model, so that all the results obtained could then be compared. As it can be seen from Tables 1 and 2, the values for the parameters $P_{low}$, and $P_{up}$ are relatively low.

**Table 1.** Results obtained by the developed PowerCollector™ model for the non-cooling experiment.

| Hours | Model Results | | Error | |
|---|---|---|---|---|
| | $P_{up}$ [W] | $P_{low}$ [W] | $P_{up}$ [%] | $P_{low}$ [%] |
| 10:00 | 44.65 | 11.41 | 6.31 | 4.92 |
| 11:00 | 55.81 | 12.22 | 11.41 | 1.83 |
| 12:00 | 60.40 | 52.44 | 11.17 | 11.57 |
| 13:00 | 58.06 | 40.25 | 10.68 | 5.92 |
| 14:00 | 62.45 | 35.72 | 2.38 | 11.66 |
| 15:00 | 78.04 | 13.23 | 4.05 | 10.25 |
| 16:00 | 77.78 | 12.78 | 2.34 | 6.50 |

**Table 2.** Results obtained by the developed PowerCollector™ model for the cooling experiment with the new orientation value.

| Hours | Model Results | | | Error | |
|---|---|---|---|---|---|
| | $P_{up}$ [W] | $P_{low}$ [W] | ΔT [°C] | $P_{up}$ [%] | $P_{low}$ [%] |
| 10:00 | 58.51 | 18.0 | 1.40 | 0,88 | 14.29 |
| 11:00 | 72.25 | 47.23 | 1.83 | 1,76 | 12.45 |
| 12:00 | 75.55 | 68.33 | 2.56 | 7,87 | 12.02 |
| 13:00 | 76.87 | 73.65 | 1.77 | 9,56 | 13.31 |
| 14:00 | 104.81 | 54.18 | 2.08 | 13,92 | 12.88 |
| 15:00 | 100.34 | 25.44 | 1.66 | 7,89 | 10.61 |
| 16:00 | 101.79 | 13.89 | 1.44 | 9,45 | 15.75 |

Further conclusions can be drawn from the analysis of all these data. The slight differences between the experimental and simulated results could be as a consequence of SolTrace inability to compute the diffuse radiation reaching the solar panels. Nevertheless, according to the overall results, the CPVT model could be considered validated.

## 4. Effects of Using Alternative Heat Transfer Fluids

After the operation analysis of the SOLARUS' CPVT in the Taguspark terrace, the next step consists of investigation the idea of using another heat-transfer fluid instead of water. The PowerCollector™ cooling system was originally designed to operate with water, which is a very common situation for most solar thermal systems [17], it has also a high-heat capacity at a constant pressure (Cp) as well as at a low cost. However, as the demand for CPVT systems increases, the enhancement of the system performance becomes a very important subject to be studied. In order to achieve this goal, one of the hypotheses currently under study is the use of nanofluids, as they have augmented thermal conductivities and a Cp similar to the water, which means that their use is expected to be very beneficial for both thermal and electrical efficiency of any CPVT system. However, they present some effects like erosion and corrosion.

### *4.1. Global Efficiency*

The first step to evaluate the nanofluids viability is related to the realization of simulations that demonstrate the potential of these fluids in terms of CPVT efficiency. In [18], for instance, an $Al_2O_3$-water nanofluid was simulated using a two-dimensional (2-D) model of a CPVT system similar to the PowerCollector™ so that the thermal and electrical energy generated could be estimated. The obtained results were then compared to the ones for the same system but with water as an HTF (Figure 7).

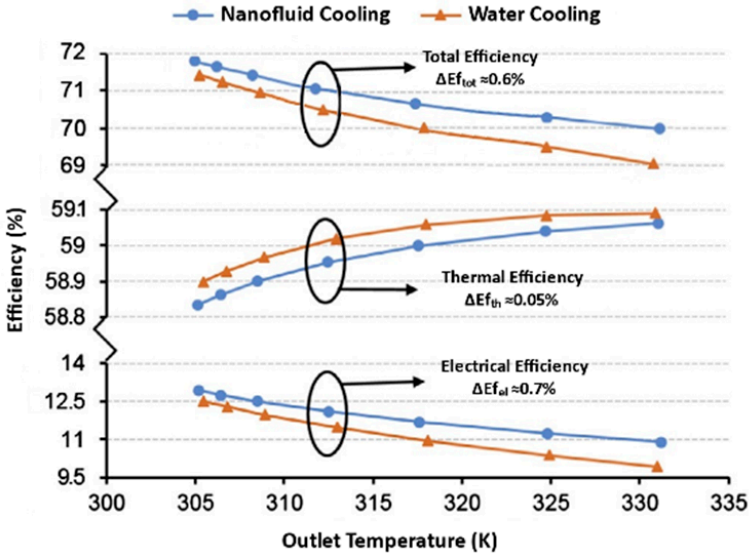


**Figure 7.** Evolution of the CPVT efficiency as a function of the outer temperature of the two heat transfer fluids under study (adapted from [18]).

Even though results show how the thermal conductivity for nanofluids can improve the electrical energy generation ($\Delta Ef_{el} \approx 0.7\%$), the same cannot be said about the thermal efficiency that, in addition to its value decrease, has a very small variation in comparison to the results of the water simulation ($\Delta Ef_{th} \approx 0.05\%$). This can be explained with the small difference between the nanofluid's heat capacity at a constant pressure (approximately 4.212 kJ/kg/K) and the water $C_p$ (approximately 4.22 kJ/kg/K). However, it should be noted that this decrease is less significant than the electrical efficiency enhancement, which makes the system global efficiency slightly higher when a nanofluid is used ($\Delta Ef_{tot} \approx 0.6\%$). Thus, with this study, it can be concluded that, in the long-run, a nanofluid-based system is preferable to a water-based one. Nonetheless, there are also other factors that are worth evaluating, like for example the deterioration of the tubes through which the nanofluid flows.

### *4.2. Corrosion and Erosion*

In order to evaluate the corrosion effect on metal surfaces, such as the aluminum of the PowerCollector™ cooling tubes, in [18–23] some experiments were carried out to determine which factors have a greater influence on this metal degradation effect. In both studies, each nanofluid has water as its base fluid, and the nanoparticles vary between $Al_2O_3$, $TiO_2$, and SiC. In the particular case of [18], all the aluminum sample targets used were exposed to similar operating conditions (fluid flow between 5 and 6 m/s and temperature ranging from 20 °C to 25 °C) during a certain period (2 to 3 weeks).

According to all the data provided in Table 3, the aluminum corrosion and erosion effects appear to be rather complex, because there are completely different results for each of the particles that are included in the nanofluids under study. These results suggest that, unlike what was to be expected, the nanoparticles present in the nanofluid do not have a major influence in the aluminum erosion. However, the nanofluid's pH seems to be the key to understand the reason behind the results described in Table 3. The aluminum, as a passive metal, has a very high corrosion resistance that results in the formation of a natural protective oxide film immediately after the exposition to air or water [21]. Hence, provided that the pH of the fluid which is in contact with the aluminum is comprised between this protective layer's stability limits (approximately between 4 and 9), the degradation effects on this metal will be minimized [22]. To prove this assumption, in [20] an experiment was carried on with the nanofluid with a pH closer to the previously mentioned stability limits. The results show a significate decrease in the erosion rate of the aluminum, which is 79.7 for the case of the nanofluid with the lowest

pH and 264 for the initial situation described in [19]. Bearing in mind that the main deterioration effects observed in the aluminum is the pitting corrosion when the fluid used on the PowerCollector™ is water [23], it can be stated that in any of the choices there will be some metal degradation effect and depending on the nanofluid used there are either advantages in using nanofluids or not.

**Table 3.** Summary of the experimental results obtained for the aluminum sample targets [18].

| Nanofluid | Observed Results Description | pH |
|---|---|---|
| $Al_2O_3$-9% | High deterioration effect, with 182 μm decrease in thickness of the area exposed to the fluid. | 8.8 |
| $Al_2O_3$-3% | Very strong corrosion effect and a considerable decrease in the sample targets thickness (263 μm). | 8.6 |
| $TiO_2$-9% | Damaging similar to the water. Incrustation of nanoparticles deposit. | 7.3 |
| SiC-3% | No significant corrosion effects when compared to water. | 5.9 |

## 5. Conclusions

The importance of studying the principle of operation of hybrid solar systems such as the PowerCollector™ is based on the need to understand all its features and specifications before considering any optimization. For this purpose, a model that portrays both the thermal and electrical behavior of this system was developed and experimentally validated. Factors such as the PV modules' tilt and orientation show a very visible effect on the amount of concentrated sunlight, which in turn proves the importance of a previous study about all the possible options for any photovoltaic setup. In the case of the one installed on the Taguspark terrace, it could be concluded that the tilt which would boost the amount of electric power throughout the year would be 15º. As for the cooling system of the PowerCollector™, comparing the obtained results for both sets of measurements (with and without the cooling technology), the advantages of including this feature are clear, since that under the conditions studied, there always seems to be a difference of about 20 W for the generated electric power. The chosen fluid to do all these experiments was water, the heat-transfer fluid for which the PowerCollector™ cooling system was originally designed to operate with. The feasibility evaluation, in terms of energy conversion efficiencies, of using other fluids other than water in a CPVT system was then included. Initially, an Al2O3-water nanofluid showed an improvement in electrical and total efficiencies, whereas the thermal efficiency slightly decreases. This demonstrates an overall efficiency enhancement in the long-run. Further studies were considered to analyze possible corrosion and erosion effects on aluminum, the PowerCollector™ cooling tubes material, due to the use of several nanofluids. A careful analysis of the data showed that the main cause for the deterioration of this metal is due to chemical corrosion caused by the fluid's pH rather than mechanical erosion by the nanofluid's solid particles. All in all, it can be concluded that it is possible to use a nanofluid in the PowerCollector™ and obtain better efficiency results instead of water. However, before any decision, there must be a previous investigation to understand which advantages and disadvantages each possible nanofluid [24] might bring.

**Author Contributions:** C.S.C. performed all the simulations and post-processing, analyzed the results, and wrote the manuscript. J.P.N.T. and J.F.P.F. analyzed the simulation results and revised the manuscript. All authors read and approved the final manuscript.

**Funding:** This research received no external funding.

**Acknowledgments:** This work was supported by FCT, through IDMEC, under LAETA, project UID/EMS/50022/2019 and under IT, project UID/EEA/50008/2019.

**Conflicts of Interest:** The authors declare no conflict of interest.

## Nomenclature

| | | |
|---|---|---|
| $P$ | Density | kg/m$^3$ |
| $C_p$ | Heat capacity | J/(kg·K) |
| $\varepsilon$ | Band Gap | eV |
| $G$ | Irradiance | W/m$^2$ |
| $H$ | Heat transfer | |
| $I_M$ | Current maximum peak power | A |
| $I_{SC}$ | Short-circuit current | A |
| $K$ | Boltzmann constant | J/K |
| $M$ | Diode ideal factor | ——— |
| $N_S$ | Number of cells in series | ——— |
| $P$ | Fluid pressure | Pa |
| $Q$ | Heat source | W/m$^3$ |
| $q$ | Heat flux | W/m$^2$ |
| $q$ | Electron charge | C |
| $T$ | Temperature | K |
| $U$ | Fluid velocity | m/s |
| $U_{MP}$ | Voltage maximum peak power | V |
| $V_\infty$ | Wind speed | m/s |
| $V_T$ | Thermal voltage | V |
| $\kappa$ | Thermal conductivity | W/(m·K) |
| $M$ | Fluid viscosity | Pa |

## References


1. Zhu, H.; Wei, J.; Wang, K.; Wu, D. Applications of carbon materials in photovoltaic solar cells. The history of solar. *Sol. Energy Mater. Sol. Cells* **2011**, *93*, 1461–1470. [CrossRef]
2. Sanjeev, J.; Soni, M.S.; Gakkhar, N. Historical and recent development of concentrating photovoltaic cooling technologies. *Renew. Sustain. Energy Rev.* **2016**, *60*, 41–59.
3. Gong, J.; Sumathy, K. Active solar water heating systems. In *Advances in Solar Heating and Cooling*; Wang, R., Ed.; Woodhead: Cambridge, UK, 2016; pp. 203–224.
4. Aberle, A.G. Surface passivation of crystalline silicon solar cells: A review. *Prog. Photovoltaics: Res. Appl.* **2000**, *8*, 473–487. [CrossRef]
5. Ward, T. *This is the Most Efficient Solar Panel Ever Made*; World Economic Forum: Cologny, Switzerland, 2017.
6. Tobergte, D.R.; Curtis, S. Concentrator Photovoltaics. Available online: http://link.springer.com/10.1007/978-3-540-68798-6 (accessed on 11 December 2018).
7. Torres, J.P.N.; Fernandes, C.A.F.; Gomes, J.; Luc, B.; Giovinazzo, C.; Olsson, O.; Branco, P.J.C. Effect of reflector geometry in the annual received radiation of low concentration photovoltaic systems. *Energies* **2018**, *11*, 1878. [CrossRef]
8. *Heat Transfer Module User's Guide*; COMSOL: Los Angeles, CA, USA, 2017; Chapter 6, pp. 431–465.
9. Torres, J.P.N.; Nashih, S.K.; Fernandes, C.A.F.; Leite, J.C. The effect of shading on photovoltaic solar panels. In *Energy Systems*; Springer: Basel, Switzerland, 2018; Volume 9, pp. 195–208.
10. Marques, L.; Torres, J.P.N.; Costa Branco, P.J. Triangular shape geometry in a Solarus AB concentrating photovoltaic-thermal collector. *Int. J. Interact. Des. Manuf.* **2018**, *12*, 1–14. [CrossRef]
11. Samuel, K.; Nashih, C.A.F.; Fernandes, J.P.N.; Torres, J.G.; Costa Branco, P.J. Validation of a simulation model for analysis of shading effects on photovoltaic panels. *J. Sol. Energy Eng.* **2016**, *138*, 044503.
12. Andreoli, M.; Torres, J.P.N.; Fernandes, C.A.F. Water dynamics simulation in the system pipes of a concentrated photovoltaic-thermal collector solar painel. *Int. J. Interact. Des. Manuf.* **2018**, *12*, 1–7. [CrossRef]
13. COMSOL. *Multiphysics Reference Manual*; COMSOL: Los Angeles, CA, USA, 2017; Chapter 13, pp. 782–786.
14. Defraeye, T.; Blocken, B.; Carmeliet, J. Convective heat transfer coefficients for exterior building surfaces: Existing correlations and CFD modelling. *Energy Convers. Manag.* **2011**, *52*, 512–522. [CrossRef]
15. Blocken, B.; Defraeye, T.; Derome, D.; Carmeliet, J. High-resolution CFD simulations for forced convective heat transfer coefficients at the facade of a low-rise building. *Build. Environ.* **2009**, *44*, 2396–2412. [CrossRef]

16. Hocksun Kwan, T.; Yao, Q. Thermodynamic and transient analysis of the hybrid concentrated photovoltaic panel and vapour compression cycle thermal system for combined heat and power applications. *Energy Convers. Manag.* **2019**, *185*, 232–247. [CrossRef]
17. Cygan, D.; Abbasi, H.; Kozlov, A.; Pondo, J.; Winston, R.; Widyolar, B.; Osowski, M. Full spectrum solar system: Hybrid concentrated photovoltaic/concentrated solar power (CPV-CSP). *MRS Adv.* **2016**, *1*, 2941–2946. [CrossRef]
18. An, W.; Zhang, J.; Zhu, T.; Gao, N. Investigation on a spectral splitting photovoltaic/thermal hybrid system based on polypyrrole nanofluid: Preliminary test. *Renew. Energy* **2016**, *86*, 633–642. [CrossRef]
19. Hamed, O.; Torabi, A.; Ahmadi, M.H.; Bahiraei, M.; Goodarzi, M.; Safaei, M.R. Application of nanofluids in thermal performance enhancement of parabolic trough solar collector: State-of-the-art. *Appl. Sci.* **2019**, *9*, 463.
20. Bubbico, R.; Celata, G.P.; D'Annibale, F.; Mazzarotta, B.; Menale, C. Experimental analysis of corrosion and erosion phenomena on metal surfaces by nanofluids. *Chem. Eng. Res. Des.* **2015**, *104*, 605–614. [CrossRef]
21. Liang, M.; Melchers, R.; Chaves, I. Corrosion and pitting of 6060 series aluminium after 2 years exposure in seawater splash, tidal and immersion zones. *Corros. Sci.* **2018**, *140*, 286–296. [CrossRef]
22. Gimenez, P.; Rameau, J.J.; Reboul, M.C. Experimental pH potential diagram of aluminium for sea water. *Corrosion* **1981**, *37*, 673–681. [CrossRef]
23. Vargel, C. *Corrosion of Aluminium*, 1st ed.; Elsevier: Amsterdam, The Netherlands, 2004.
24. Abd El-Samie, M.M.; Ju, X.; Xu, C.; Du, X.; Zhu, Q. Numerical study of a photovoltaic/thermal hybrid system with nanofluid based spectral beam filters. *Energy Convers. Manag.* **2018**, *174*, 686–704. [CrossRef]

© 2019 by the authors. Licensee MDPI, Basel, Switzerland. This article is an open access article distributed under the terms and conditions of the Creative Commons Attribution (CC BY) license (http://creativecommons.org/licenses/by/4.0/).